Experimental study on the separation of silica gel supports by gravitational field-flow fractionation
II. Sample preparation, stop-flow procedure and overloading effect

Jiří Pazourek*, Josef Chmelík

Institute of Analytical Chemistry, Academy of Sciences of the Czech Republic, Veveří 97, CZ-611 42 Brno, Czech Republic

Abstract

Two kinds of silica were studied: a commercial porous chromatographic support with a broad size distribution and a special non-porous silica with a very narrow size distribution. The preparation of sample suspensions in aqueous solution of the non-ionic detergent Tween 60 was optimized and the influence of the amount of particles injected and of the stop-flow time on separation was investigated. A study of the overloading effect showed a dramatic increase in the mean retention ratio with increasing amount of particles. Considering previous observations, an explanation of the overloading effect in gravitational field-flow fractionation is suggested.

1. Introduction

Gravitational field-flow fractionation (GFFF) belongs to the family of field-flow fractionation (FFF) techniques where an external force field acts perpendicularly to a carrier liquid flow with a non-uniform velocity profile. Concentration profiles of sample components result from the applied field and the component properties and directly determine the elution times. GFFF utilizes the Earth's gravity as the external force field which drives analyte particles (usually micrometre-sized particles because of the relatively weak field) towards the channel bottom that is placed horizontally (accumulation wall). However, there are other forces acting on particles in the

flow, viz., hydrodynamic lift forces. In contrast to gravity, they can drive the particles away from the channel accumulation wall. The retention ratios observed are usually higher than those calculated on the basis of the simple steric model that presumes the particles to roll on the accumulation wall. This means that lift forces cause the focusing (hyperlayer) elution mode [1,2]. The vertical position of the zones in the flow velocity profile is determined by the particle size and density because the gravitational force (the mass) depends on the size and density, and hydrodynamic lift forces depend on the size. GFFF has been applied to the separation and characterization of various particulate materials, e.g. glass, silica gel and latex beads [3–8] and blood cells [9,10].

Particulate samples in FFF cannot be consid-

* Corresponding author.

ered as point-like, having no interactions among themselves or with the accumulation wall. The influence of particle–particle and particle–wall interactions on retention behaviour has been studied [8,11,12]. However, even without such interactions, the retention behaviour differs from ideal behaviour because of the finite sample concentration. Increasing samples concentration causes deviations of the sample concentration profile and flow velocity profile from their ideal infinite dilution limits: Hoyos and Martin [13] made a detailed analysis of the influence of finite concentration on retention in sedimentation FFF (SdFFF). They explained theoretically previous observations [14] on tailing and increases in retention ratio with increasing amount of sample (polystyrene latex beads of diameter of 460 nm). However, as they noted, the model cannot be applied in the focusing separation mode.

This paper is the second part of a study examining the separation and characterization of silica gel particles by GFFF; the first part [8] dealt with the selection of an optimum carrier liquid and characterization of the lift forces activity in GFFF. The aim of this part was to find an optimum means of sample preparation (preparation of suspensions of particulate materials) and to explain the effect of overloading, both of which are prerequisites to interpreting GFFF experiments.

2. Experimental

2.1. Equipment

The experimental arrangement was described elsewhere [6–8]. The separation channel was cut in an 80-μm spacer, which was placed between two mirror-quality float glass plates and clamped between two Plexiglas blocks. The channel had dimensions 20 × 360 mm (dead volume 0.53 ml). The inlet and outlet triangles of the channel had heights of 3 cm. The pump was an HPP 4001 (Laboratory Instruments, Prague, Czechoslovakia). A UVM 4 spectrophotometric detector (Development Workshops, Prague, Czechos-

lovakia) was used at 265 nm (optical path 5.7 mm).

2.2. Materials

The samples were non-porous silica gel spheres of diameter 1.43 ± 0.01 μm (a kind gift from Professor E. Kováts, SFIT Lausanne, Switzerland, denoted here as 1.4-μm particles) and a sample of commercial porous silica of diameter 4.78 ± 1.12 μm (Tessek, Prague, Czech Republic, denoted here as 5-μm particles). Their sizes were determined by electron microscopy. The sample suspensions were of concentration 0.025–200 mg/ml. The carrier liquid was a 0.1% solution of Tween 60 (Fluka, Buchs, Switzerland) in distilled water with final density 1.00 g/ml.

3. Results and discussion

3.1. Sample preparation

The most common procedure for the preparation of suspensions is homogenization of the particulate material in a detergent solution. The detergent prevents concentration of the solid particles on interfaces during manipulation (sampling, injection, transport through the channel). However, porous materials suspended in liquids (such as common silica gel supports) can contain gas cavities on the particle surface. Problems with such samples can arise not only because of worse wetting but also because the cavities influence the apparent density, which directly affects the retention ratio observed. Giddings and Moon [15] concluded that suspensions of porous silica particles contained air activities even after sonication for 6 h. Therefore, we verified three methods of preparation of porous silica samples.

Fractogram A in Fig. 1 was obtained from a sample prepared by simply putting porous 5-μm silica particles in a 0.1% aqueous solution of Tween 60 and shaking. Fractogram B was recorded after 5 min of sonication of the suspension of the same composition and fractogram C
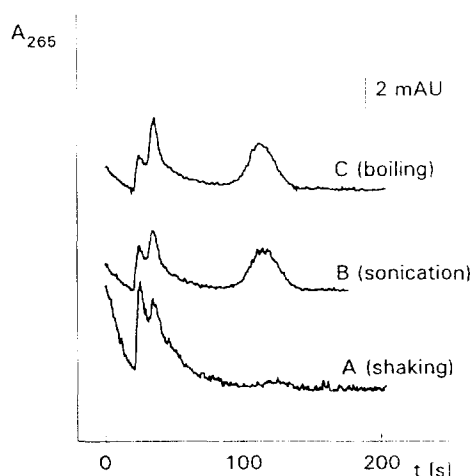
Fig. 1. Optimization of sample preparation procedure. Samples were porous 5-μm silica gel particles of concentration 1 mg/ml in a 0.1% solution of Tween 60. Fractogram A, recorded after shaking the silica powder in the suspension medium only; B, sample after 10 min of sonication; C, sample after 15 min of boiling, tempering and following 1 min of sonication. Flow-rate, 0.99 ml/min; volume injected, 1 μl.

after 15 min of boiling, following tempering and 1-min sonication of a silica particle suspension in 0.1% Tween 60. It is obvious that the retained peak in fractogram A is almost hidden in an anomalousy 'noisy' baseline. This is probably a result of chaotic elution of badly wetted particles having a broad particle density distribution while after sonication of the suspension this density distribution was reduced and the retained peak was well pronounced (fractogram B). No significant changes in peak dispersion or retention ratio in fractogram C were observed after boiling, which should release contingent cavities, so we concluded that sonication in the detergent solution was an adequate as the sample preparation procedure for the samples used, and in all subsequent experiments we used suspensions of silica particles in 0.1% Tween 60 prepared only by 1-min sonication.

3.2. Stop-flow procedure and relaxation

The relaxation in FFF usually reduces and non-equilibrium contribution to the total peak dispersion because during the relaxation time (in the absence of the carrier liquid flow) the analyte is expected to form an equilibrium concentration profile suitable for subsequent elution. However, in experiments with particulate samples, the process of sedimentation has to be taken into account. After the sample injection into a channel, the particles are randomly distributed across the whole channel thickness. If the carrier liquid flow is not interrupted, then the particles in the upper and central planes migrate at higher velocities than those located closer to their equilibrium positions near the accumulation wall. This is a consequence of the parabolic flow profile. The particles injected into the upper channel region must pass through the central region because they also sediment. Therefore, the initial sample distribution causes a distinction of elution velocities and thereby contributes to peak broadening. In order to avoid these effects, one has to use either a special split or frit inlet system [16,17] or a stop-flow procedure. In the stop-flow procedure, the sample is injected at a reduced flow-rate and in this way is introduced into the rectangular region of the channel spacer (just behind the spacer inlet triangle). Then the flow is stopped and the sample is affected only by the external field. Finally, the flow is resumed at the elution flow-rate.

In our system, we stop the flow to let the particles settle (to reach a sedimentation equilibrium) in order to reduce their vertical distribution before the elution. This strategy follows from the analysis of the lift forces function [7,18]: in the absence of any external field acting perpendicularly to the flow direction, there are three equilibrium positions across the channel thickness where particles can be focused during the elution owing to hydrodynamic lift forces activity: expressed in dimensionless distance δ denoting the relative distance of a particle center from the channel bottom, the three positions are 0.19, 0.50 and 0.81, respectively. This would mean that particles of the same size and density could be focused in three different positions (and consequently they could exhibit different retention ratios, namely 1 and 1.5) if they have been distributed randomly across the whole channel thickness at the beginning of elution. A similar

conclusion holds (there are three distinguished retention ratios as a maximum) if an external field (e.g., gravitational) acts [8]. This means that in GFFF not only peak dispersion but also the retention time is influenced by the initial sample distribution and thus experimental data are not always easy to interpret. In order to simplify the interpretation, it is advantageous to stop the flow after the injection and to let the sample particles settle to the accumulation wall. The time period without flow can be termed the stop-flow time rather than the relaxation time as it was described above that the procedure does not form a concentration profile of particles kept during subsequent elution; the settled particles have only the same starting position. When the flow is reapplied, the hydrodynamic forces drive the particles off the accumulation wall to an equilibrium position where the lift forces are exactly balanced by the gravitational forces. This equilibrium position cannot be reached without the carrier liquid flow (before the elution). The same starting point of all particles is advantageous because identical particles reach their equilibrium positions at the same rate and have the same mean velocity along the channel. A time period necessary for the vertical movement of the particles from their starting position to their equilibrium position (induced by the lift forces) can be called the relaxation time. It has been found previously that this time is relatively short (a few seconds) [7,8,19].

The theoretical time for the settlement of 1.4-μm particles (calculated as the sedimentation time of the particle across the channel height) is 50 s. In order to observe any influence of the stop-flow time, we performed experiments at high flow-rates when the retention time was comparable to this stop-flow time (Fig. 2). Without any flow interruption, the particles eluted from the channel in an asymmetric peak with a left edge retention ratio of 1.5 and a tail overlapping the position of $R = 1$ ($t_0 = 6.4$ s); no retained peak was observed (see Fig. 2, fractogram A). In fractogram B in Fig. 2, one can see a retained peak. This means that particles reached a suitable position within 10 s of the stop-flow time. After longer stop-flow times we obtained
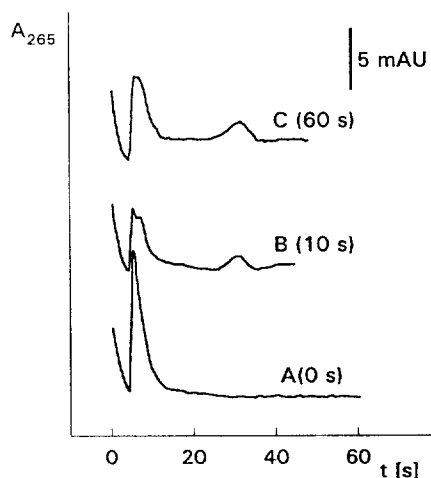

Fig. 2. The stop-flow procedure. The time at each fractogram shows the proper stop-flow time. Experimental conditions: sample, 1.4-μm silica gel particles of concentration 0.25 mg/ml; volume injected, 1 μl; flow-rate, 5.00 ml/min.

retained peaks with the same retention ratio and dispersion as shown in fractogram C for 60 s. This means that it is not necessary to wait for the complete sedimentation time. It seems that it is sufficient if the particles reach the lower half of the channel where they will be focused during subsequent elution under the influence of the lift and gravitational forces.

3.3. Overloading

We also studied the influence of the sample volume and concentration on the retention. In Fig. 3 are shown overlapped fractograms obtained with 1.4-μm particles at two constant concentrations with variable injection volumes. It is evident that an increase in injection volume causes a decrease in the mean retention time and an increase in the peak dispersion by tailing. A similar evolution of series of peaks was observed with 5-μm particles (data not shown). In Fig. 4 are displayed fractograms of 5-μm particles recorded at two constant injection volumes and variable concentrations. One can see that an increase in concentration results in a decrease in the mean retention time which is similar to the observations shown in Fig. 3. Analogous fractog-
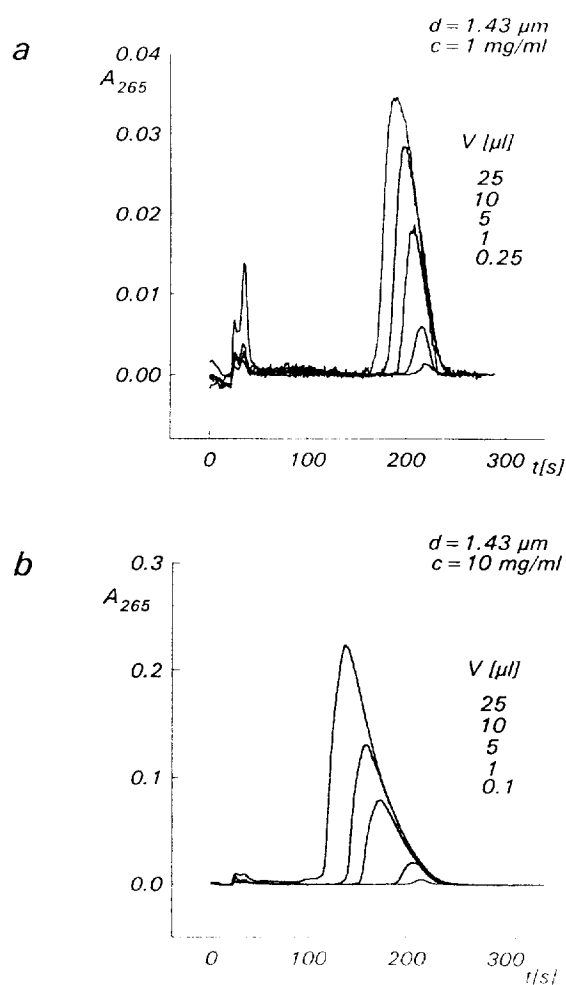
a

a

Fig. 3. Overloading effects in GFFF at constant sample concentration. The V values are the volumes injected; the smaller the volume, the smaller is the peak maximum. Concentrations of 1.4-μm silica gel suspension, (a) 1 and (b) 10 mg/ml; flow-rate, 0.99 ml/min.

b

b

Fig. 4. Overloading effects in GFFF at constant sample volume. The c values are the concentrations of sample injected; the lower the concentration, the smaller is the peak maximum. Volumes of 5-μm silica gel suspension, (a) 1 and (b) 10 μl; flow-rate, 0.49 ml/min.

rams were obtained at 1.4-μm particles (data not shown).

Previous observation on overloading effects in FFF showed various results: fronting of peaks and a decrease in retention ratio (the sample was polystyrene of molecular mass 200 000–670 000), or tailing and a decrease in retention ratio (the sample was polystyrene of molecular mass 860 000) in flow FFF [20]. In experiments with SdFFF, Kirkland et al. [21] reported an increase
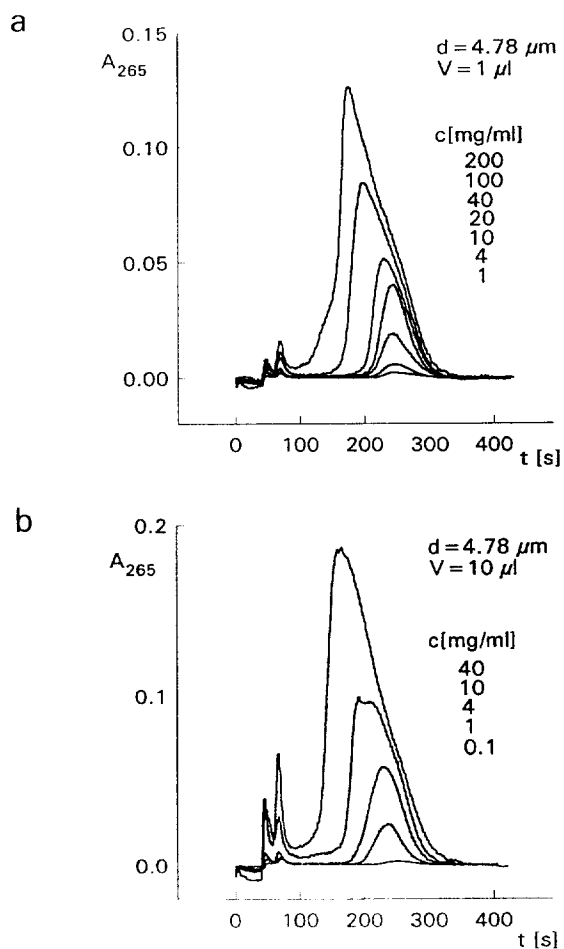
in retention ratio with constant peak width (polystyrene latex beads of diameter 176 nm).

As is obvious from our GFFF experiments, we observed tailing peaks and an increase in retention ratio, which is in contrast to the above-mentioned observations of other workers. A key to understanding this is a difference in separation modes: whereas under normal conditions (with an exponential concentration distribution [20,21]) samples of nanometre size are pressed towards the accumulation wall and the hydro-dynamic lift forces are not pronounced, in our

experiments particles >1 μm are focused in zones above the channel bottom much higher than presumed from simple steric exclusion.

Moreover, we observed a similar evolution of peak characteristics (i.e., an increase in the retention ratio and tailing) for both variable concentration at a constant sample volume and vice versa. This behaviour implies that the retention is determined mainly by the product of concentration and volume (cV), i.e., the number of particles, rather than by the concentration or volume of the sample. We tried to confirm this idea by comparing experiments performed with constant product cV. Fig. 5 shows fractograms of 5-μm silica and Fig. 6 similar fractograms for 1.4-μm silica, all obtained at $cV = 1$ μg. It is clear that the peaks in each triad are virtually identical, although the concentrations or volumes differ even 40-fold for both kinds of particles.

An explanation of the observed increase in retention ratio with increasing number of particles can be based on the course of the lift forces function (see Fig. 7). The magnitude of the lift forces is highest at the channel bottom and then rapidly decreases. Because we examined only retained peaks $(R < 1)$, the zones were always focused between the channel bottom and the position $\delta = 0.19$. During the elution process,
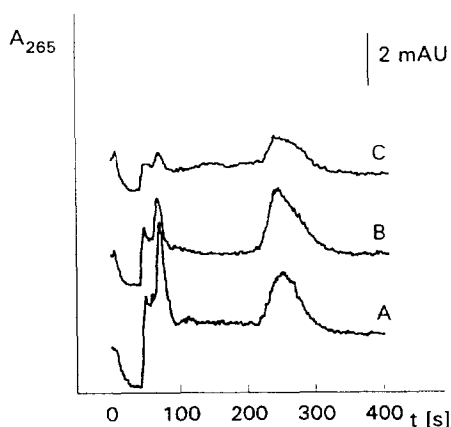

Fig. 6. Fractograms of 1.4-μm particles obtained at constant flow product $cV = 1$ μg. Fractogram A, $c = 0.1$ mg/ml and $V = 10$ μl; B, $c = 1$ mg/ml and $V = 1$ μl; C, $c = 10$ mg/ml and $V = 0.1$ μl. Flow-rate, 0.99 ml/min.

particles oscillate around their equilibrium position δ_0 where the magnitude of the lift forces F equals the Archimedes mass of particles $G = \pi d^3 g \Delta\rho / 6$ (d is the particle diameter, g is gravitational acceleration and $\Delta\rho$ is the density difference between particles and carrier liquid). Particles in a lower position $\delta_1 < \delta_0$ are pushed back upward to the equilibrium position faster $(F_1 \gg G)$ than those from the upper positions $\delta_2 > \delta_0$ $(F_2 < G)$. Hence the particles occupy the upper positions in higher numbers, so the zone centre of gravity exhibits a higher mean velocity (a higher retention ratio) because of the parabolic flow profile. This mechanism can also explain our observations in Figs. 5 and 6, where the same numbers of particles exhibited the same retention ratio and peak dispersion independently of the injected volume/concentration.

A conclusion following from our explanation is that overloading effects in GFFF are minimized if the experiments are carried out with the minimum number of particles.

Fig. 5. Fractograms of 5-μm particles obtained at constant product $cV = 1$ μg. Fractogram A, $c = 0.1$ mg/ml and $V = 10$ μl; B, $c = 1$ mg/ml and $V = 1$ μl; C, $c = 4$ mg/ml and $V = 0.25$ μl. Flow-rate, 0.49 ml/min.
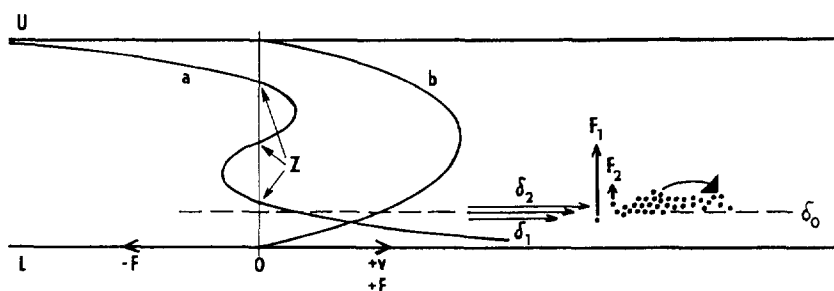
Acknowledgement

Fig. 7. Schematic representation of overloading effects in GFFF channel. U and L represent the upper and lower channel walls, curves a and b represent the courses of the lift forces and flow velocity profile, respectively, $-F$ and $+F$ show the orientation of the lift forces and $+v$ shows the direction of the carrier liquid flow. The dashed line δ_0 represents the location of the particle equilibrium position where $F = G$, and Z denotes three positions inside the channel where $F = 0$ (δ is the dimensionless distance of a particle centre from the channel bottom and equals 0.19, 0.50 and 0.81, respectively). Three arrows represent the streamlines near the particle equilibrium position: the middle arrow is at the position δ_0 where $F = G$ and corresponds to the retention ratio of very diluted samples, the bottom arrow is at the position $\delta_1 < \delta_0$ where $F_1 \gg G$ and particles are rapidly transported to the equilibrium position and the top arrow is at the position $\delta_2 > \delta_0$ where $F_2 < G$ and the velocity of the carrier liquid flow is higher. Hence these particles move faster along the channel than the particles at δ_0 and it is the cause of the observed increase in the mean retention ratio.

References

[1] J.C. Giddings, Sep. Sci. Technol., 18 (1983) 765.
[2] J. Janča and J. Chmelík, Anal. Chem., 56 (1984) 2481.
[3] J.C. Giddings and M.N. Myers, Sep. Sci. Technol., 13 (1978) 637.
[4] J.C. Giddings, M.N. Myers, K.D. Caldwell and J.W. Pav, J. Chromatogr., 185 (1979) 261.
[5] K.D. Caldwell, T.T. Nguyen, M.N. Myers and J.C. Giddings, Sep. Sci. Technol., 14 (1979) 935.
[6] J. Pazourek, P. Filip, F. Matulík and J. Chmelík, Sep. Sci. Technol., 28 (1993) 1859.
[7] J. Pazourek and J. Chmelík, Chromatographia, 35 (1993) 591.
[8] J. Pazourek, E. Urbánková and J. Chmelík, J. Chromatogr., 660 (1994) 113.
[9] P.J. Cardot, J. Gerota and M. Martin, J. Chromatogr., 93 (1991) 568.
[10] E. Urbánková, A. Vacek, N. Nováková, F. Matulík and J. Chmelík, J. Chromatogr., 583 (1992) 27.

[11] M.E. Hansen and J.C. Giddings, Anal. Chem., 61 (1989) 811.
[12] Y. Mori, K. Kimura and M. Tanigaki, Anal. Chem., 62 (1990) 2668.
[13] M. Hoyos and M. Martin, Anal. Chem., 66 (1994) 1718.
[14] M.E. Hansen, J.C. Giddings and R. Beckett, J. Colloid Interface Sci., 132 (1989) 300.
[15] J.C. Giddings and H.M. Moon, Anal. Chem., 63 (1991) 2869.
[16] S. Lee, M.N. Myers and J.C. Giddings, Anal. Chem., 61 (1989) 2439.
[17] M.K. Liu, P.S. Williams, M.N. Myers and J.C. Giddings, Anal. Chem., 63 (1991) 2115.
[18] V.L. Kononenko and J.K. Shimkus, J. Chromatogr., 520 (1990) 271.
[19] P.S. Williams, Sep. Sci. Technol., 29 (1994) 11.
[20] K.D. Caldwell, S.L. Brimhall, Y. Gao and J.C. Giddings, J. Appl. Polym. Sci., 36 (1988) 703.
[21] J.J. Kirkland, W.W. Yau and W.A. Doerner, Anal. Chem., 52 (1980) 1944.